JOURNAL OF CATALYSIS 24, 446–459 (1972)

The Kinetics of Adsorption of Carbon Tetrachloride and Chloroform from Air Mixtures by Activated Carbon

LEONARD A. JONAS*

Research Laboratories, Edgewood Arsenal, Maryland 21010

AND

W. J. SVIRBELY

University of Maryland, College Park, Maryland 20742

Received April 27, 1971

The kinetics of gas adsorption were studied in an air flow apparatus using CCl_4 and $CHCl_3$ as the adsorbate vapors and activated carbon as the adsorbent. Five fractions of uniformly activated carbon granules, in size ranges of 0.130 to 0.036 cm diam, were packed in glass columns to various bed depths and weights, and subjected at several temperatures to a 0.1 relative pressure of the adsorbate vapor at various fixed flow velocities. On plotting the ratio of exit to inlet vapor concentrations against time, sigmoid shaped curves were obtained at all flow rates, carbon weights, and granule diameters. Vapor breakthrough of the bed was taken as the time when 1% of the inlet concentration appeared in the exit flow stream, $(C_x/C_0) = 0.01$.

The Wheeler adsorption equation was used to analyze the experimental data for a fixed temperature at this breakthrough time (t_b). The adsorption rate constant at this breakthrough time was first order with respect to gas molecules and essentially independent of carbon granule diameters. The values were 4000 min^{-1} and 7255 min^{-1} at 25°C for CCl_4 and $CHCl_3$, respectively.

The sigmoid curve for the complete breakthrough of CCl_4 was found to contain three adsorption rate constants. The pseudo first-order constant was operative when the concentration of active sites was much larger than the concentration of gas molecules $(0 < C_x/C_0 < 0.04)$; a second-order rate constant was operative when active sites and concentrations of gas molecules were both affecting the rate $(0.04 < C_x/C_0 < 0.65)$; and a pseudo first-order rate constant with respect to active sites when the concentration of gas molecules was much greater than active sites $(0.65 < C_x/C_0 < 0.95)$. Arguments are advanced to explain the variation of the rate constants between large and small carbon granules in terms of a combined mechanism which involves internal diffusion and surface adsorption.

Introduction

Many studies have been made on the thermodynamic properties involved in the physical adsorption of gaseous adsorbates by adsorbents, as evidenced by the massive literature (*1*) on the subject of heterogeneous adsorption equilibria. However, relatively fewer studies have concentrated on the adsorption kinetics, especially at the breakthrough time. Mathematical equations and kinetic processes describing the process of gaseous adsorbate removal based on a mass balance which assumes that the quantity of gas sent into

* Abstracted in part from a thesis submitted by L. A. Jonas to the Graduate Faculty of the University of Maryland in partial fulfillment of the requirements for the degree of Doctor of Philosophy.

an adsorbent bed could be related with the quantity adsorbed by the bed are in the literature (*2*).

A different approach to the kinetics of gas adsorption by beds of adsorbent granules has been made by Wheeler (*3*). Four basic differential equations were derived which described concurrent gas adsorption phenomena in a bed and which required simultaneous solution. By means of various simplifying assumptions, the four equations were reduced to one total differential equation

$$-dF/d\lambda = (k_v/V_L)F\psi(F), \qquad (1)$$

whose solution was

$$-\int \frac{dF}{F\psi(F)} = \frac{k_v\lambda}{V_L} + \text{constant}, \qquad (2)$$

where λ was the bed thickness, V_L the superficial velocity, k_v the adsorption rate constant, F the ratio C_x/C_0 (which under steady-state conditions was also equal to W/W_e), and $\psi(F)$ a function of W/W_e, the ratio of the amount of gas adsorbed to the maximum amount capable. To evaluate the constant in Eq. (2), a continuity equation of mass balance per unit area was set up, namely, mass of vapor into bed equals mass of vapor adsorbed plus mass of vapor penetrating, or

$$C_0V_Lt_b = \rho_B\int_0^\lambda W(x)\,dx + V_L\int_0^t C(\lambda)\,dt, \qquad (3)$$

where C_0 was the inlet concentration in g/cm^3, $C(\lambda)$ the concentration as a function of bed depth λ (cm) at any time t_b (min), V_L the superficial linear velocity of the gas-air mixture (cm/min), ρ_B the bulk density of the adsorbent bed (g/cm^3), and $W(x)$ the grams of vapor adsorbed per gram of adsorbent at a point x in the bed. If the whole bed were brought into adsorption equilibrium (saturated) in time t_b, the weight adsorbed per unit area would be $\rho_BW_e\lambda$, where W_e was the weight (g/g) in equilibrium with C_0, the inlet concentration. From Eqs. (2) and (3) the breakthrough equation for an adsorbent bed of granules, for small ratios of C_b/C_0 and for steady state flow and removal processes in the bed, was derived as

$$t_b = [(\rho_BW_e)/(C_0V_L)] \times \left\{\lambda - \frac{V_L}{k_v}\ln[K(C_0/C_b)]\right\}, \qquad (4)$$

where k_v was the rate constant (min^{-1}) for the adsorption process, C_b the breakthrough concentration (g/cm^3), and K a factor depending on the shape of the adsorption isotherm obtained mathematically in the derivation as an integration constant. For an arbitrarily fixed ratio of $C_b/C_0 = 0.01$ we make the assumption (*4*) that $K = 1$.

In this paper, we report on the ability of Eq. (4) to describe the adsorption of CCl_4 and $CHCl_3$ by activated carbon at the breakthrough time under conditions of fixed C_0, C_b, ρ_B, and of varying carbon granule diameter, temperature, λ, and V_L.

Vapor adsorption isotherms run on the BPL grade Lot 6098 activated carbon (*5*) for CCl_4 and for $CHCl_3$ at 25, 40, and 60°C, are shown in Fig. 1. The curves show the usual Type 1 shape and also the expected decrease in volume of vapor adsorbed at a fixed pressure as the temperature increased. The curves also show that the linear portions of the isotherms are covered by an extremely small range of vapor pressure. This sharp, steep rise is due to the high activation of the carbon granules. From an experimental point of view, it would be exceedingly difficult to maintain temperature control in a flow system sufficiently close to assure a constant inlet gas concentration within the linear portion of the isotherm. Because temperature control at 25°C to within ±1°C would not significantly affect the inlet vapor concentration on the plateau of the isotherm, we chose to confine our experimental work to the plateau region. Consequently, the relative pressure for the vapors tested was set at 0.1; i.e., at 25°C, the mean inlet vapor concentrations were 98.6 mg/liter and 128.9 mg/liter for CCl_4 and $CHCl_3$, respectively.

Papers (*6*) have appeared in the literature over the past number of years on the dynamics of fluid flow entering and exiting a column. However, the mathematical relations derived have been based on the assumption that the concentration of the ad-

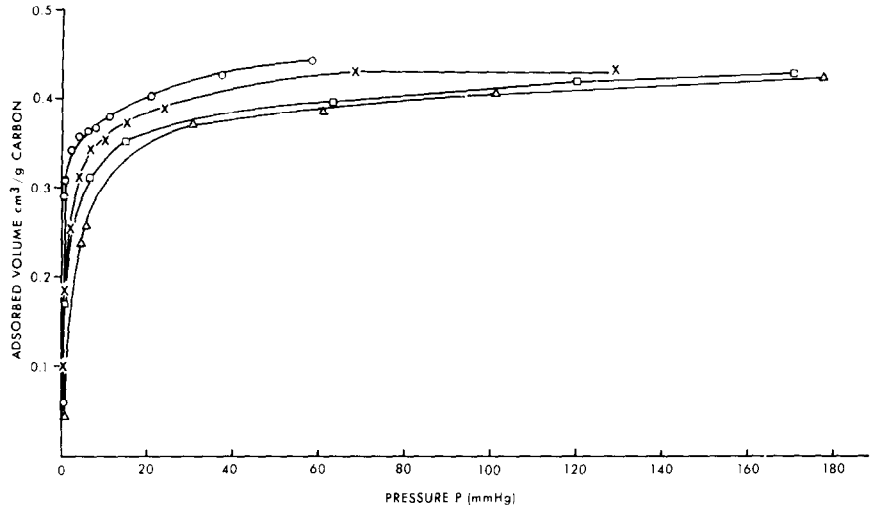

FIG. 1. Vapor adsorption isotherms on activated carbon: ○, CCl_4 at 20°C; ×, $CHCl_3$ at 25°C; □, $CHCl_3$ at 40°C; △, $CHCl_3$ at 60°C.

sorbable vapor was low enough so that a linear isotherm pertained, a restriction which we could not meet experimentally. Consequently, we made no attempt to check the validity of such mathematical equations through use of our data.

MATERIALS AND APPARATUS

Activated carbon. A granular carbon adsorbent, BPL grade, Lot No. 6098, manufactured by Pittsburgh Activated Carbon Co. from bituminous coal was used. One hundred gram batches of the granular carbon were sieved into five mesh fractions, corresponding to mean granule diameters of 0.130, 0.102, 0.072, 0.055, and 0.036 cm, respectively.

Carbon tetrachloride. Reagent ACS grade, Allied Chemical Company.

Chloroform. Reagent ACS grade, Allied Chemical Company.

Pyridine. (For Karl Fischer Reagent) Eastman Organic Chemicals Company.

Chromosorb W. Solid support for PE 154-D gas chromatograph column, hexamethyldisilizane treated, 60–80 mesh, Johns-Manville Product Company.

Carbowax 20M. Stationary phase (liquid coating on solid support) dissolved in chloroform before coating the Chromosorb W. The weight ratio of Carbowax 20M to Chromosorb W was 1 to 11. Johns-Manville Products Co.

Solutions. Two solutions of carbon tetrachloride in pyridine containing 314.4 mg and 6.329 mg CCl_4 per ml and two solutions of chloroform in pyridine containing 313.5 mg and 6.270 mg $CHCl_3$ per ml, respectively, were prepared and used as calibration standards for the fractometer.

Chromatograph. The experimental data were obtained using a Perkin-Elmer 154-D Vapor Fractometer detecting the chlorinated hydrocarbon vapor by a thermal conductivity cell. The 90″ × ¼″ column for the PE 154-D was packed with 8.3% Carbowax 20M on Chromosorb W. The recorder was operated at a chart speed of 2 in./min. The traced area on the recorder chart was converted into a quantity of vapor penetrating the bed by referring to the calibration curve previously determined and then into a vapor concentration in units of g/cm³.

Vapor test apparatus. The apparatus was made of glass tubing fitted together with standard taper and ball-socket joints. The apparatus had three functional sections, one for vapor generation, another for vapor adsorption by the carbon, and the third for the detection of the carbon. Specific features of the apparatus were the generation of a vapor from a liquid and its

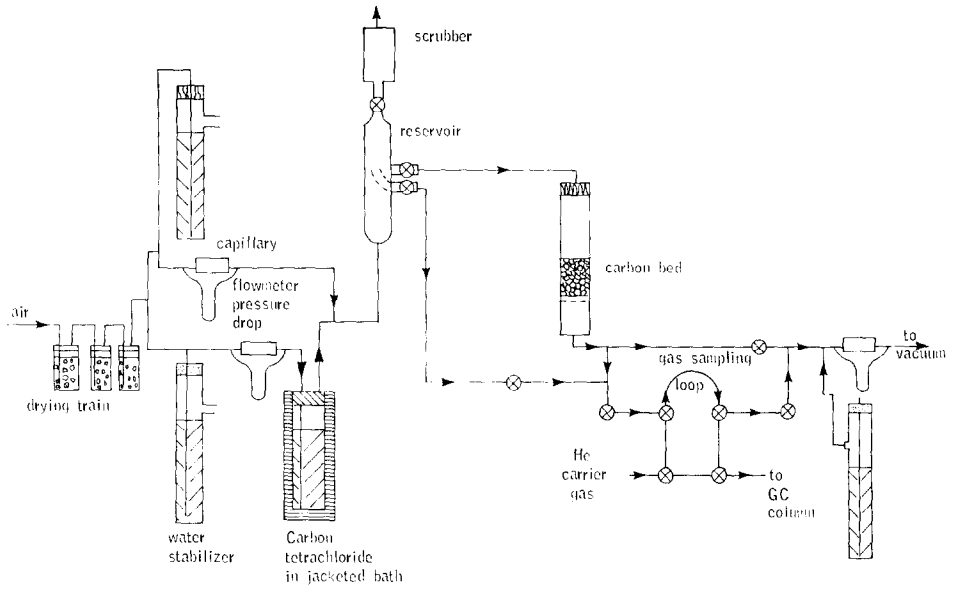

FIG. 2. Schematic of vapor test apparatus.

dilution with pure air to any desired concentration, the range of carbon bed depths and area exposed to a known vapor concentration, and the control of the vapor-air flow rate into the carbon bed. A schematic of the test apparatus is shown in Fig. 2.

EXPERIMENTAL

Compressed air was cleaned and dried by passage through three tubes connected in series, each of which contained packed glass wool and Drierite. This clean dry air was then split into two parts, one sweeping across a liquid layer of carbon tetrachloride or chloroform and becoming saturated with adsorbate vapor, and the second part meeting the air-adsorbate vapor stream at a right angle and diluting the adsorbate vapor concentration. The stream of vapor and air was then directed to a glass reservoir at a flow rate of 4 liter/min. The reservoir contained two sampling ports closed with 8 mm glass stopcocks. One port was used to determine the concentration of adsorbate vapor in the air mixture; the other port to withdraw this vapor concentration at a known flow rate through a fixed bed of activated carbon to determine its penetration rate through the bed. The system requirement was that the withdrawal flow rate be equal to or less than the generating flow rate.

The packed beds of activated carbon granules were prepared by dropping the granules into the adsorption column by a free fall of 122 cm. Two adsorption columns with inside cross-sectional areas of 0.833 and 4.23 cm^2, respectively, and were used with a $\frac{1}{8}$" coarse glass frit, the former column when packed with carbon granules having 0.036, 0.055, and 0.072 cm diam, and the latter when packed with the 0.102 and 0.130 cm granules. The carbon granules packed on top of the glass frit with uniform and reproducible densities dependent upon the mean granule diameter and the inside diameter of the adsorption column.

The air flow rates used in the apparatus were rigidly controlled by adjusting the pressure differential of a manometer which measured the pressure gradient across the specific glass capillary tube used to control the air flow.

The PE154-D gas chromatograph was used both to determine the inlet vapor concentration and to monitor the rate of vapor penetration of the packed bed of carbon granules. The gas sampling valve (GSV) of the chromatograph, having a fixed volume

of 5 cm³ was inserted in series with the air-vapor mixture being drawn into the carbon bed and positioned between the bed and the vacuum source. The GSV, therefore, constantly sampled any chlorinated hydrocarbon vapor penetrating the carbon bed as the test proceeded.

The vapor penetration rate was determined as a function of carbon weight, flow rate, granular diameter, and temperature. The mean inlet vapor concentrations for CCl_4 and $CHCl_3$ were 98.6 mg/liter of air and 128.9 mg/liter of air, respectively, representing a relative pressure of 0.102 at 25°C ± 1°C. The exit flow from the carbon bed passed constantly through the GSV, the contents of which were flushed with helium into the gc column every 53 sec when CCl_4 was the adsorbate vapor. The test was completed when the area trace on the chart indicated that the full inlet concentration was penetrating the carbon bed without noticeable attenuation, showing that the carbon granules were no longer capable of adsorbing vapor. The adsorption column containing the vapor saturated carbon was weighed before being dumped, thus providing a direct weight method for calculating the saturation capacity of the carbon for the vapor.

After the traced areas on the chart were converted to vapor quantities, a plot was made of the ratios of exit concentration, C_x, to the inlet concentration, C_0, against the sampled time t for each specified run. The plots of C_x/C_0 vs t were sigmoid shaped curves differing in the slopes of the convex, straight, and concave segments of the curves. Figure 3 illustrates such a plot.

For chloroform, because of the higher column retention time, the exit concentration was sampled every 70 sec.

The procedure for testing the adsorption of the carbon bed at 35 and 50° was essentially the same as that at 25°, except that provision was made for heating the outside of the glass adsorption column which surrounded the carbon bed.

Results and Discussion

A. *Adsorption Characteristics at 1% Concentration Penetration*

1. Modified Wheeler equation. Wheeler's Eq. (4) can be transformed, for $K = 1$, into Eq. (5)

$$t_b = \frac{W_e}{C_0 Q}\left[W - \frac{\rho_B Q \ln(C_0/C_x)}{k_v} \right], \quad (5)$$

where Q was the volume flow rate

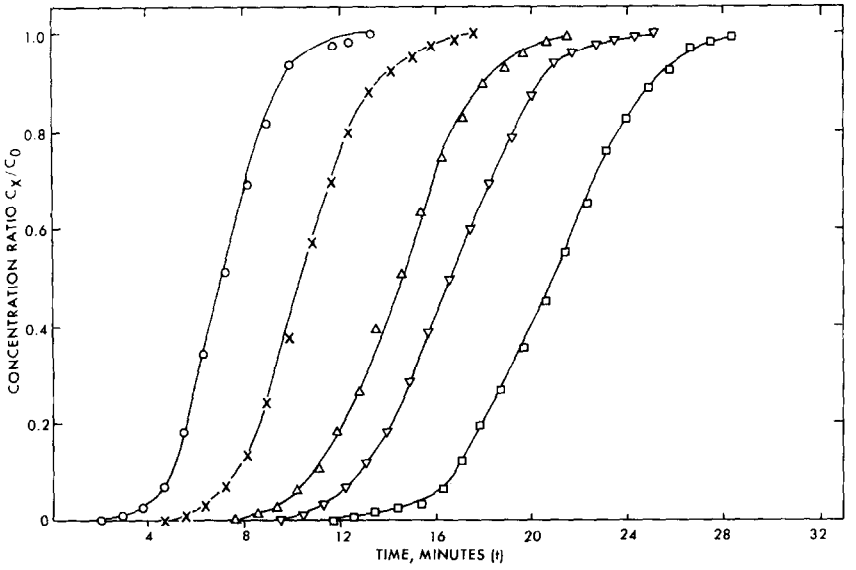

Fig. 3. CCl_4 penetration curves for various weight carbon beds: 0.130 cm diam granules: 1220 cm³/min flow rate: 25°C: ○, 1.49 g; ×, 2.12 g; △, 3.04 g; 3.63 g; □, 4.29 g.

(cm^3/min) equal to the product of area A (cm^2) and superficial linear velocity V_L (cm/min), and $\rho_B Q \ln(C_0/C_x)/k_v$ equal to W_c, the critical bed weight or that value of W when $t_b = 0$.

2. Penetration time vs bed weight. The penetration or breakthrough time (7), t_b, was defined as the time at which 1% of the inlet concentration appeared in the stream ($C_b/C_0 = C_x/C_0 = 0.01$). Values of t_b at the breakthrough time were obtained from the sigmoid curves for each of the specified conditions. The values of t_b were then plotted against carbon bed weights for each of the flow rates for each of the granule sizes in accord with Eq. (5). Straight line curves were obtained. Figure 4 illustrates such a plot for CCl_4 at 25°C using 0.055 cm diam granules.

3. Saturation capacity and rate constant. The kinetic capacity W_e, in gram vapor adsorbed per gram activated carbon, and the first-order adsorption rate constant k_v, in min^{-1}, were calculated from the slopes and the x-axis intersections of the lines obtained by plotting t_b vs W from Eq. (5). The calculated results are listed in Table 1 and shown graphically in Fig. 5. Reference to Fig. 5* shows that k_v is essentially independent of granular size over the size range used. Also, it is observed that for a granular size of 0.072 cm or less, the kinetic saturation capacity no longer depends on granular size. Total saturation capacities, W_m, obtained by weighing the completely saturated carbon beds at complete concentration breakthrough, i.e., $C_x/C_0 = 1.0$, are listed in Table 2. On examining the data for the 0.055 cm granules, it is evident that its W_e value of 0.669 g CCl_4/g carbon at C_x/C_0 of 0.01 represents 98.2% of its maxi-

TABLE 1

CCl_4 KINETIC SATURATION CAPACITY AND RATE CONSTANT AT 1% CONCENTRATION BREAKTHROUGH AS A FUNCTION OF CARBON GRANULE DIAMETER

d_p Granule diam (cm)	Q Flow rate (cm^3/min)	M Slope (min/g)	W_e Saturation capacity (g/g)	W_c Critical bed wt (g)	k_v Rate constant (min^{-1})
0.130	430	8.696	0.367	0.220	3655
	600	5.911	0.332	0.270	4156
	900	4.274	0.378	0.460	3659
	1220	3.366	0.391	0.560	4074
			Mean 0.367		
0.102	430	11.11	0.473	0.200	3922
	600	7.632	0.441	0.275	3980
	900	5.116	0.451	0.400	4104
	1220	3.822	0.460	0.550	4046
			Mean 0.456		Mean 3950
0.072	430	13.64	0.592	0.234	3665
	600	11.09	0.671	0.310	3860
	900	7.600	0.690	0.440	4080
	1220	5.576	0.686	0.590	4124
			Mean 0.660		
0.055	430	15.50	0.659	0.210	3904
	600	10.63	0.636	0.275	4160
	900	7.444	0.678	0.385	4290
	1220	5.773	0.703	0.550	4230
			Mean 0.669		Mean 4040
					Overall Mean 4000

* Plotted as granular volume, assuming granule sphericity.

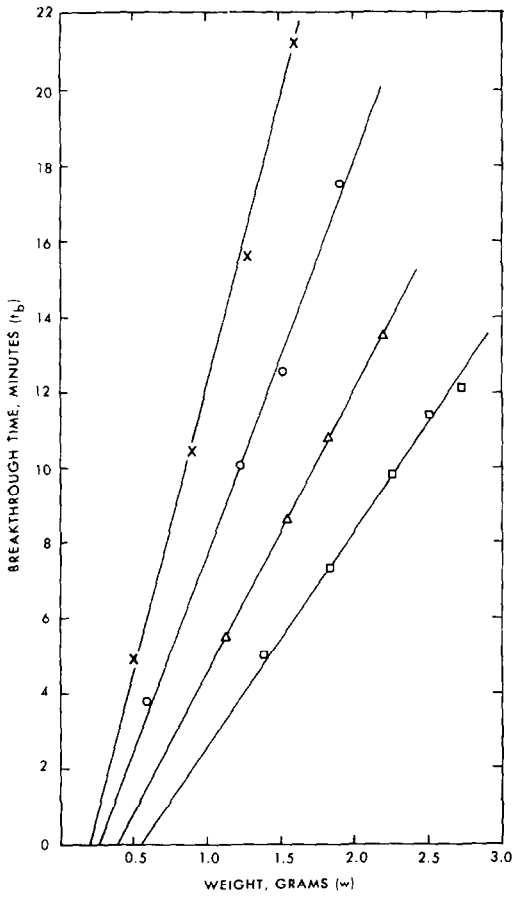

FIG. 4. CCl_4 breakthrough time as a function of carbon weight for 0.055 cm diam granules: 25°C: ×, 430 cm³/min; ○, 600 cm³/min; △, 900 cm³/min; □, 1220 cm³/min; bulk density, 0.414 g/cm³.

mum possible capacity attainable at complete saturation, indicating that for the remaining range of $0.01 < C_x/C_0 \leq 1.0$ very little more CCl_4 can be adsorbed. For our largest granule, namely 0.130 cm diam, the W_e/W_m value is 62%.

4. Penetration time vs residence time. The residence time, τ, for a vapor in a bed of carbon granules is defined as

$$\tau = \lambda/V_L. \tag{6}$$

Since $W = \lambda A \rho_B$ and $Q = AV_L$, then Eq. (6) can be rewritten as

$$\tau = \frac{W}{Q\rho_B}. \tag{7}$$

Values of τ were calculated at the various flow rates for each bed weight. On plotting values of penetration time, t_b, as ordinate against the corresponding residence time, τ, as abscissa, four linear plots are obtained which tend to converge at a common x-axis intercept corresponding to $t_b = 0$ and $\tau = \tau_c$. We conceive τ_c to be a critical residence time. The value of τ_c was 0.00105 min.

TABLE 2
CCl_4 TOTAL SATURATION CAPACITY OF CARBON GRANULES AT COMPLETE CONCENTRATION BREAKTHROUGH: WEIGHT METHOD

W_m Total saturation capacity, g/g			
Granule diam 0.055 (cm)	Granule diam 0.072 (cm)	Granule diam 0.102 (cm)	Granule diam 0.130 (cm)
0.704	0.659	0.618	0.597
0.711	0.682	0.619	0.591
0.690	0.673	0.620	0.593
0.688	0.665	0.618	0.595
0.697	0.644	0.615	0.589
0.675	0.645	0.615	0.585
0.673	0.675	0.602	0.604
0.693	0.674	0.619	0.607
0.697	0.665	0.604	0.588
0.675	0.665	0.612	0.609
0.683	0.669	0.633	0.594
0.682	0.655	0.615	0.604
0.688	0.638	0.615	0.597
0.698	0.664	0.623	0.585
0.651	0.654	0.621	0.582
0.654	0.661	0.607	0.580
0.661	0.658	0.621	0.573
0.656	0.662		0.572
0.667	0.669		0.580
	0.665		0.571
Mean	Mean	Mean	Mean
0.681	0.662	0.617	0.590

One can transform Wheeler's Eq. (5) into Eq. (8), namely,

$$t_b = (W_e\rho_B/C_0)[(W/Q\rho_B) - (1/k_v)\ln(C_0/C_x)]. \tag{8}$$

By analogy with Eqs. (5) and (7), it is evident that the critical residence time τ_c can be identified in Eq. (8) as

$$\tau_c = \frac{1}{k_v}\ln\left(\frac{C_0}{C_x}\right). \tag{9}$$

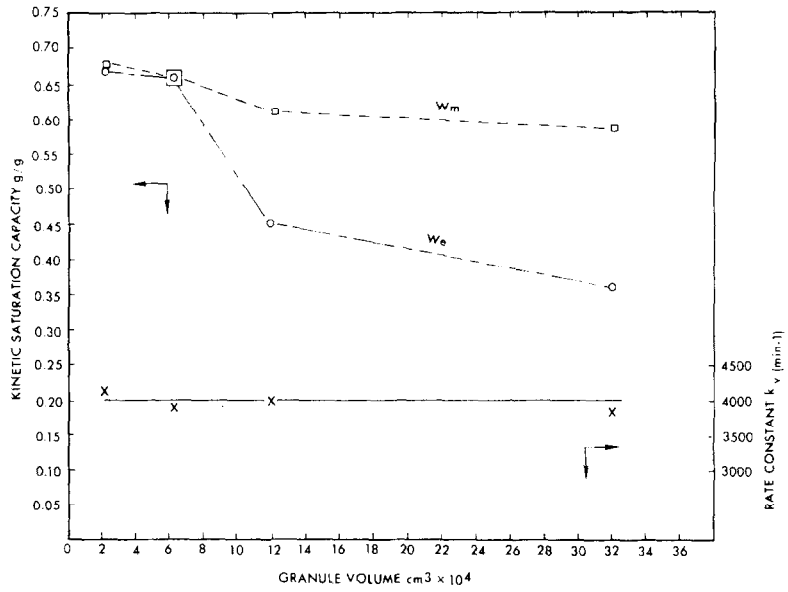

FIG. 5. CCl_4 saturation capacity and rate constant as a function of carbon granule volume: 25°C: □, capacity at 100% concentration penetration; ○, capacity at 1% concentration penetration; ×, rate constant at 1% concentration penetration.

5. Effect of granular diameter. Using the values of the adsorption rate constant and kinetic saturation capacity determined from tests on the above carbon granule diameters, it was deemed worthwhile to see if one could predict the breakthrough time for smaller granular diameters and check the results with experimental measurements. For this purpose experimental data were obtained on 0.036 cm diam carbon granules at a flow rate of 430 cm³/min. The kinetic saturation value, W_e, was taken as 0.67 g/g based on the 0.055 diam data. With C_0, Q, ρ_B, C_0/C_b, k_v equal to 0.0000986 g CCl_4/cm³, 430 cm³/min, 0.395, 100, and 4000 min^{-1}, respectively, values of t_b were calculated at several values of W through use of Eq. (8) and compared with the experimental data. The agreement was excellent and these results are shown in Table 3.

TABLE 3

CCl_4 BREAKTHROUGH TIME AS A FUNCTION OF CARBON WEIGHT FOR 0.036 CM DIAM GRANULES

W Carbon wt (g)	τ Residence time (min)	t_b Breakthrough time (min)	
		Calculated	Experimental
0.422	0.00248	3.8	3.6
0.605	0.00356	6.6	6.6
0.773	0.00455	9.2	8.9

6. Effect of temperature. The breakthrough time, t_b, for 1% of the inlet vapor concentration penetrating the carbon bed was determined for various bed weights of 0.055 cm diam granules with carbon tetrachloride and chloroform at several temperatures. The experimental data for both vapors are shown in Table 4. Saturation capacities, critical weights and adsorption rate constants were calculated as already discussed. These data are shown in Table 5. It is apparent that the rate constant decreases markedly with an increase in temperature.

7. Mechanism and thermodynamic aspects. If one assumes that the adsorption mechanism can be represented by the process

$$V + S \underset{k_2}{\overset{k_1}{\rightleftarrows}} V \cdot S, \qquad (10)$$

TABLE 4
BREAKTHROUGH TIME AS A FUNCTION OF CARBON WEIGHT[a] FOR 0.055 CM DIAM GRANULES: 444 CM³/MIN @ 35°C; 466 CM³/MIN @ 50°C; 437 CM³/MIN @ 30°C

Temp (°C)	Vapor	W Carbon wt (g)	τ Residence time (min)	t_b Breakthrough time (min)
35	CCl_4	0.584	0.00317	5.1
		0.690	0.00375	6.2
		0.867	0.00471	10.1
		1.007	0.00547	12.1
		1.262	0.00686	15.5
50	CCl_4	0.702	0.00364	2.1
		0.902	0.00467	4.4
		1.049	0.00544	6.1
		1.197	0.00620	7.0
		1.418	0.00735	10.1
30	$CHCl_3$	0.88	0.00477	7.9
50	$CHCl_3$	0.548	0.00284	1.3
		0.689	0.00357	4.2
		1.054	0.00546	6.3
		1.361	0.00706	7.5
		1.292	0.00670	8.7

[a] Mean bulk density was 0.414 g/cm³.

then the rate of the process is given by the following equation

$$-d(V)/dt = k_1(V)(S) - k_2(V \cdot S), \quad (11)$$

where (V), (S), and $(V \cdot S)$ represent concentrations of adsorbable vapor, unoccupied active sites, and occupied sites, respectively. Since in the discussion so far we have been concerned with the situation when the number of active sites is large compared to the incoming vapor molecules, i.e., $(S) \gg (V)$, we can rewrite the rate equation as

$$-d(V)/dt = k_1'(V) - k_2(V \cdot S). \quad (12)$$

Material balance shows that

$$(V_0 - V) = (V \cdot S), \quad (13)$$

so Eq. (12) becomes

$$-d(V)/dt = (k_1' + k_2)(V) - k_2(V_0). \quad (14)$$

If k_2 is markedly less than k_1', then pseudo first-order kinetics would appear, a fact which we have experimentally established. The equilibrium constant, K_L, can be defined in terms of the adsorption rate constant k_1' (or k_v) and the desorption rate constant k_2 by

$$K_L = k_v/k_2. \quad (15)$$

The temperature study on vapor adsorption, discussed in the previous section, was made using the 0.055 cm diam granules, which no longer showed the kinetic saturation capacity to be dependent on granular size (Section A–3). Thus intragranular diffusion cannot be considered rate controlling for this granular size and adsorption can take place as rapidly as the gas molecules are transported by bulk (gas) diffusion to the granule. Accepting this argument, the relationship between the adsorption rate constant k_v and the equilibrium constant K_L (dimensionless) was defined as

$$k_v = K_L D_G/A, \quad (16)$$

where A is the cross-sectional area in cm² and D_G is the gas diffusion coefficient for the adsorbed vapor in cm²/min. Values of

TABLE 5
CARBON ADSORPTION PROPERTIES FOR CCl_4 AND $CHCl_3$ AT 1% PENETRATION: 0.055 CM DIAM GRANULES AT VARIOUS TEMPERATURES

	CCl_4			$CHCl_3$	
Carbon properties	25°C	35°C	50°C	25°C	50°C
Saturation capacity, g/g	0.669	0.662	0.466	0.616	0.428
Critical weight, g	0.205	0.264	0.505	0.113	0.264
Ads rate constant, min⁻¹	4000	3207	1759	7255	3367
Diffusion coeff cm²/min	4.266	4.632	4.974	4.704	5.484
Equilibrium constant	781	577	295	1290	511

TABLE 6
THERMODYNAMIC PARAMETERS FOR GAS ADSORPTION

Vapor	$\Delta H°$ (cal/mole)	$\Delta G°$ (cal/mole) 25°C	35°C	50°C	$\Delta S°$ @25°C (cal/mole °K)
CCl_4	−7510	−3950	−3890	−3650	−11.9
$CHCl_3$	−7040	−4240	—	−4000	−9.39

D_G were first calculated by use of Gilliland's Equation (*8*). Then values of K_L were calculated by use of Eq. (16). Results are tabulated in Table 5. Values of $\Delta H°$, $\Delta G°$ and $\Delta S°$ were calculated in the usual way through use of Eqs. (17), (18), and (19), respectively.

$$\frac{d \log K_L}{d(1/T)} = -\frac{\Delta H°}{4.58}, \tag{17}$$

$$\Delta G° = -RT \ln K_L, \tag{18}$$

$$\Delta G° = \Delta H° - T\Delta S°. \tag{19}$$

The results of these calculations are shown in Table 6.

The values of $\Delta H°$ for CCl_4 adsorption and $CHCl_3$ adsorption were −7510 cal/mole and −7040 cal/mole, respectively. These values for the heats of adsorption compare quite closely with the literature values for heats of liquefaction of −7230 cal/mole for CCl_4 and −6910 cal/mole for $CHCl_3$. Small but finite difference between the larger adsorption heats and smaller liquefaction heats are shown by Brunauer (*9*) to be characteristic of vapors whose isotherm at low pressure is concave to the pressure axis (Type 1).

B. *Adsorption Characteristics at Complete Breakthrough*

1. Dimensionless sigmoid curve. As already mentioned when the vapor penetration of carbon beds is followed from initial to complete breakthrough and the ratio of exit to inlet concentration is plotted against time a sigmoid curve (2g, 5b, 5e) is obtained. Furthermore, for a fixed inlet concentration, temperature, and carbon granule diameter the exit concentration was a function of carbon bed weight and flow rate. The curve for any one size carbon granule diameter can be generalized by plotting the dimensionless concentration parameter (ratio of exit to inlet concentration, C_x/C_0) against a dimensionless time parameter (ratio of time of test to vapor residence time in the bed, t/τ. Such a plot should show the approach to saturation or exhaustion of the activated carbon.

The times at which various exit to inlet concentration ratios occurred were determined for each of the four carbon granular fractions and the dimensionless time ratios were then obtained by dividing by the residence time of the vapor in the bed. For any one carbon granule diameter, the time ratios were independent of carbon weight and flow rate, since the residence time τ itself is an explicit function of these parameters. In view of the fact, however, that the saturation capacity was dependent upon granule size for the two larger diameter granules (0.130 and 0.102 cm) but essentially independent of the size for the two smaller sizes (0.072 and 0.055 cm), the data for the two larger sizes and for the two smaller sizes were separately averaged. These data are plotted in Fig. 6. The curves show the expected longer time for initial bed penetration and the expected steeper slope for the smaller granules. Furthermore, there is a convergence of the two curves at a time ratio of about 3600. When the curves are interpreted as the rate of exhaustion of the carbon beds, the convergence of the curves represents the approach to equilibrium saturation of the carbon for the vapors, a valid reason for the independence of granular diameter at the convergence point.

2. Adsorption rate constants. The curves shown in Fig. 6 consist of three major line segments. Each line segment represents a

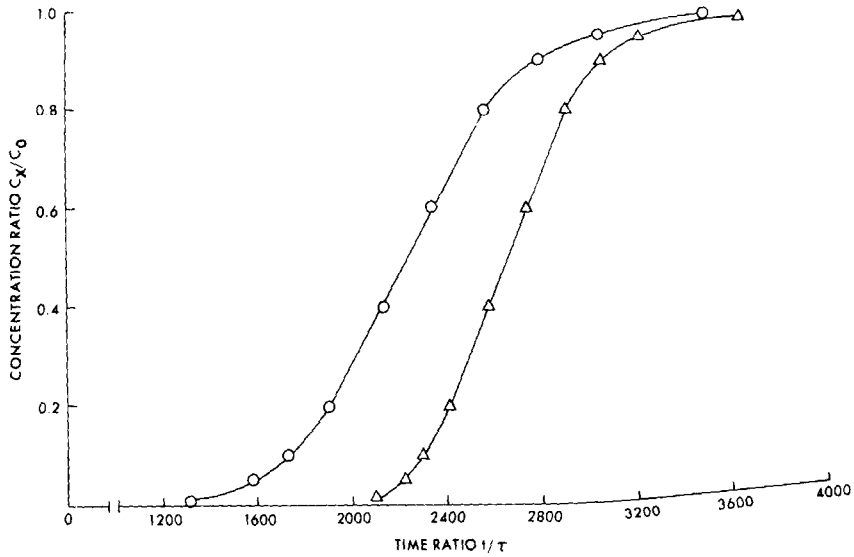

FIG. 6. Dimensionless concentration as a function of dimensionless time for various carbon granule diameters: ○, 0.130 and 0.102 cm diam; △, 0.072 and 0.055 cm diam.

different rate at which gas has penetrated the carbon bed, starting with the first slow change of exit concentration with time, the second segment showing a linear relation between C_x/C_0 and t/τ, and the third segment the slow approach of C_x/C_0 toward its limiting value of 1. We have extracted adsorption rate constants from the three line segments through the use of a model for concentration change.

(a) Model for concentration change. The carbon granule is viewed as surrounded by a volume of space within which a specific concentration of gas exists starting with the inlet concentration, C_0, at $t = 0$. As adsorption of the gas in this surrounding volume proceeds with time, the number of gas molecules per unit volume capable of being adsorbed also decreases. The rate of this decrease is the rate of gas adsorption and its concentration dependence determines the order.

(b) Active sites for adsorption. If CCl_4 molecules were to be placed on a surface the closest approach of one molecule to another, assuming a cross-sectional area of 36.7×10^{-16} cm^2 per molecule and no interactions, would result in 2.7×10^{14} molecules per cm^2. On the assumption that one gas molecule is adsorbed onto one active site, there would then be a maximum of 2.7×10^{14} active sites per cm^2. Hayward and Trapnell (*10*) state that on the average 10^{15} active sites per cm^2 exist on a clean metal surface. Since the activated carbon had an internal pore area of 1058 m^2/g, there could be a maximum of 2.86×10^{21} active sites per gram of carbon. Assuming that all the sites were available for CCl_4 adsorption, it would be possible for 2.86×10^{21} CCl_4 molecules to be adsorbed per gram of carbon. The mean inlet concentration of 0.986×10^{-4} g CCl_4/cm^3 air at 25°C is equivalent to 3.9×10^{17} CCl_4 molecules/cm^3 of air.

(c) Rate of gas concentration change. The rate of gas concentration decrease can be calculated for the generalized sigmoid curve as follows:

(1) Transform Eq. (7) into Eq. (20), namely,

$$t/\tau = (tQ\rho_B)/W. \qquad (20)$$

The real time t in minutes is calculated for the following standard conditions: weight $W = 1$ g; volume flow rate $Q =$ 1000 cm^3/min; bulk density $\rho_B = 0.401$ g/cm^3 for the 0.130 and 0.102 cm diam granules and $\rho_B = 0.424$ g/cm^3 for 0.072 and 0.055 cm diam granules.

(2) Calculate the values of t for specific C_x/C_0 values from the correspond-

ing t/τ values by use of Eq. (20). For example, for the larger diameter granules at a C_x/C_0 value of 0.01, the t/τ value is 1312 and the calculated t value is 3.27 min. This leads to a calculated value of 12.75×10^{20} molecules of CCl_4 adsorbed. Since at $t = 0$, there were 2.86×10^{21} active sites, there now remain 15.85×10^{20} active sites. This stepwise procedure was continued at various increasing values of C_x/C_0.

In Fig. 7 plots are shown of $1/C - 1/C_0$ vs t over the C_x/C_0 range of 0.01–0.80 in accordance with the usual procedure for a second-order reaction when both reactants are present in equal concentrations. The resulting straight line curves for both large and small diameter carbon granules spanned most but not all of the data points plotted, and therefore the straight lines were drawn only through the range over which second-order kinetics were applicable. The slopes of the lines were obtained from a regression analysis of the data. These slopes represent the second-order rate constants and were equal to 2.19×10^{-22} (active sites/g)$^{-1}$ min^{-1} for the large diameter granules and 5.49×10^{-22} (active sites/g)$^{-1}$ min^{-1} for the small diameter granules. Furthermore, an analysis of the lines showed that second-order kinetics pertained over the $1/C - 1/C_0$ range of 3.50–8.00 and 8–15.50 for the small and large diam granules, respectively. By back calculation these numbers correspond to a C_x/C_0 range of 0.04–0.60 and 0.03–0.65 for the large and small diameter granules, respectively.

These second-order rate constants in units of (active sites/g)$^{-1}$ min^{-1} were converted to the more familar units of (moles/

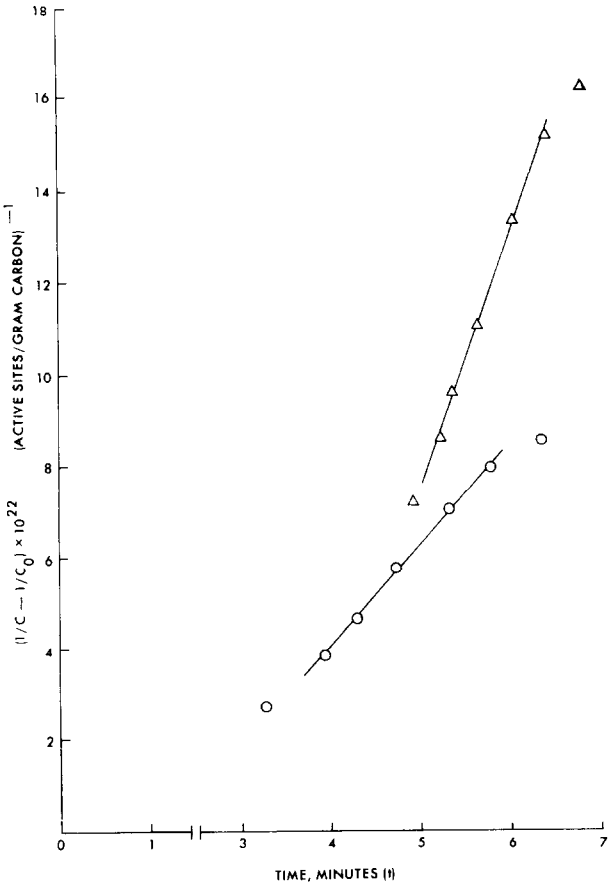

FIG. 7. Second-order kinetics for CCl_4 adsorption: ○, 0.130 and 0.102 cm diam granules; △, 0.072 and 0.055 cm diam granules; drawn lines, computer regression lines.

TABLE 7
CCl_4 Adsorption Rate Constants for Large and Small Diam Carbon Granules

Range	Kinetics	CCl_4 Adsorption rate constant	
		0.130 and 0.102 cm diam carbon granules	0.072 and 0.055 cm diam carbon granules
$0 < C_x/C_0 \leq 0.04$	Pseudo first order wrt gas molecules	3950 min^{-1}	4040 min^{-1}
$0.04 < C_x/C_0 \leq 0.65$	Second order	$0.186\left(\frac{moles}{liter}\right)^{-1}min^{-1}$	$0.441\left(\frac{moles}{liter}\right)^{-1}min^{-1}$
$0.65 < C_x/C_0 \leq 0.95$	Pseudo first order wrt active sites	0.032 min^{-1}	0.054 min^{-1}

liter)$^{-1}$ min^{-1} (see Appendix) and are listed in Table 7.

It was believed that for C_x/C_0 values greater than 0.65 the density of active sites was rapidly decreasing and, therefore, beyond this point one should observe pseudo first-order kinetics with respect to active sites. Figure 8 shows the graphical method usually used for testing first-order kinetics. The C_x/C_0 range of 0.70–0.95 was used. The slopes of the lines were obtained from equations obtained by a regression analysis and the rate constants were calculated from the slopes. The results are listed in Table 7.

Since gas adsorption by a fixed bed of carbon granules begins as a pseudo first-order process with respect to gas molecules and ends, with the carbon approaching saturation, as a pseudo first-order process with respect to *vacant* active sites, it is evident that a crossover period must exist when the densities of gas molecules and active sites becomes approximately equal. During this time period, shown in Fig. 7 to be short in duration, second-order kinetics prevail. The sigmoid curve shows this in general as the straight line portion of the curve.

When complete saturation occurs, the bed becomes transparent to the inlet gas concentration and the rate constant of gas adsorption is reduced to zero.

3. Nature of diffusion mechanism. Reference to Table 7 shows that each of the rate constants applicable to the three exit concentration ranges in the complete breakthrough curve is greater to some degree for the small diam granules than for the larger ones. In the sequential steps of external (bulk) diffusion, internal (intraparticle) diffusion, and surface adsorption, a significantly slow intraparticle diffusion step would manifest itself in an increased overall rate constant for the small granule compared to the large ones. There is some

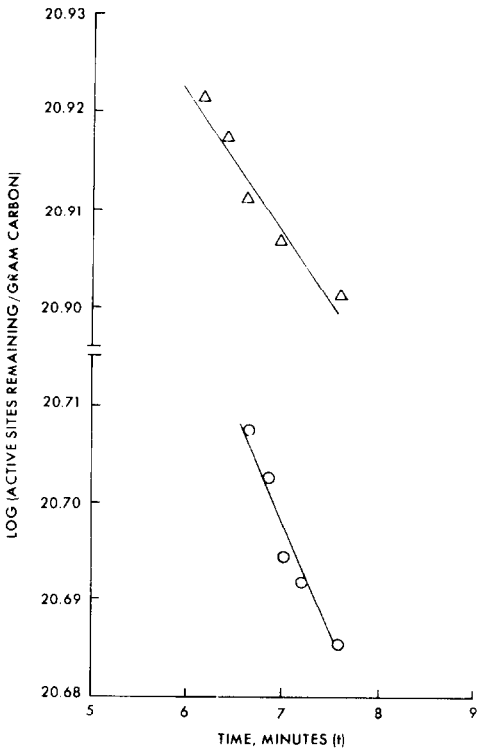

FIG. 8. Concentration of carbon active sites for CCl_4 adsorption as a function of time: △, 0.130 and 0.102 cm diam granules; ○, 0.072 and 0.055 cm diam granules; drawn lines, computer regression lines.

evidence for this condition, since we show in Fig. 5 that the kinetic saturation capacity W_e is a function of carbon granule size and it does not reach its maximum value until the carbon granule is 0.072 cm diam or smaller. Masamune and Smith (*11*) in a study of the adsorption of nitrogen by beds of porous vycor particles have reported that internal diffusion processes determined the overall rate for particles larger than 0.02 cm diam. In the study of the adsorption of ethane on silica gel, Schneider and Smith (*6e*) have reported that for particles 0.01 cm diam the contribution of internal diffusion and surface adsorption to the overall rate constant was in the ratio of 55–45; whereas for particles 0.05 cm diam the ratio was 95–4.

Accepting our results to be outside experimental error, we conclude that a combination of internal diffusion and surface adsorption is the controlling mechanism. Evidence for combined mechanisms being rate controlling has been shown before (*12*).

Appendix

Conversion of (active sites/gram carbon)$^{-1}$ min^{-1} to (moles/liter)$^{-1}$ min^{-1}:

$$2.19 \times 10^{-22} \left(\frac{\text{active sites}}{\text{gram carbon}}\right)^{-1} \text{min}^{-1} \cdot \left(\frac{0.401 \text{ g carbon}}{\text{cm}^3}\right)^{-1} \cdot \left(\frac{1000 \text{ cm}^3}{\text{liter}}\right)^{-1} \cdot \left(\frac{1 \text{ active site}}{\text{gas molecule}}\right) \cdot \left(\frac{6.02 \times 10^{23} \text{ gas molecules}}{\text{mole}}\right) \cdot \left(\frac{0.566 \text{ liters air}}{\text{liter carbon}}\right)^{*} = 0.186 \left(\frac{\text{moles}}{\text{liter}}\right)^{-1} \text{min}^{-1}.$$

* Volume void fraction of packed bed of carbon granules.

References

1. (*a*) Brunauer, S., "The Adsorption of Gases and Vapors," Princeton University Press, Princeton, NJ, 1943; (*b*) Young, D. M., and Crowell, A. D., "Physical Adsorption of Gases," Butterworths, Washington, D. C., 1962.
2. (*a*) Bohart, G., and Adams, E., *J. Amer. Chem. Soc.* **42**, 523 (1920); (*b*) Short, O. A., and Pierce, F. G., MITR No. 114, Proj. DA-1-11(1946); (available in Technical Library, Edgewood Arsenal, MD and MA Inst. of Tech., Cambridge, MA); (*c*) Klotz, I. M., and Feurenbacher, J. B., OSRD Report No. 5239, Part I, (1944) (Technical Library, Edgewood Arsenal); (*d*) Klotz, I. M., Fehrenbacher, J. B., McCabe, W. L., Johnson, V., Roake, W. E., Cutforth, H. G., and Thomas, J. W., OSRD Report No. 5239, Parts II and III, (1945); (*e*) Gamson, B. W., Thodos, G., and Hougen, O. A., *Trans. Amer. Inst. Chem. Eng.* **39**, 29 (1943); (*f*) Hougen, O. A., and Watson, K. M., *Ind. Eng. Chem.* **35**, 537 (1943); (*g*) Klotz, I. *M., Chem. Rev.* **39**, 241 (1946); (*h*) Mecklenburg, W., *Z. Elektrochem.* **31**, 488 (1925); *Kolloid Zh.* **52**, 88 (1930); (*i*) Danby, C., Davoud, J., Everett, D., Hinshelwood, C., and Lodge, R., *J. Chem. Soc.* **1946**, 918; (*j*) Amundson, N. R., *J. Phys. Colloid Chem.* **52**, 1153 (1948); **54**, 812 (1950); (*k*) Thomas, H. C., *NY Acad. Sci. Ann.* **49**, 161 (1948).
3. Wheeler, A., private communication.
4. For the case of nonselective vapor poisoning of catalysts and conversion of feed before breakthrough, Eq. (7) of publication "Wheeler, A., and Robell, A. J., *J. Catal.* **13**, 299 (1969)" can be transformed into this form.
5. Bulletin PAC 1064, Type BPL Granular Carbon, Pittsburgh Activated Carbon Co.
6. (*a*) Thomas, H. C., *J. Chem. Phys.* **19**, 1213 (1951); (*b*) Rosen, J. B., *J. Chem. Phys.* **20**, 387 (1952); (*c*) Underhill, D. W., *Nucl. Appl.* **6**, 544 (1969); (*d*) Underhill, D. W., *Nucl. Appl. Technol.* **8**, 255 (1970); (*e*) Schneider, P., and Smith, J. M., *AIChEJ.* **14**, 762 (1968).
7. Hiester, N. K., and Vermeulen, T., *Chem. Eng. Progr.* **48**, 506 (1952).
8. Perry, J. R., "Chemical Engineers Handbook," 4th edition, p. 14-20, McGraw-Hill Book Co., New York, 1963.
9. Brunauer, S., "The Adsorption of Gases and Vapors," p. 232, Princeton University Press, Princeton, NJ, 1943.
10. Hayward, D. O., and Trapnell, B. M. W., "Chemisorption," p. 18, Butterworths, London, 1964.
11. Masamune, S., and Smith, J. M., *AIChEJ.* **10**, 246 (1964).
12. (*a*) Masamune, S., and Smith, J. M., *AIChE J.* **11**, 34 (1965); (*b*) Rosen, J. B., *Ind. Eng. Chem.* **46**, 1590 (1954).